International Journal of Latest Research in Science and Technology
Volume 3, Issue 5: Page No 29-33. September-October 2014
https://www.mnkpublication.com/journal/ijlrst/index.php

ISSN (Online):2278-5299

PROPERTIES OF FABRICATED AL DOPED ZnO NANORODS BY SPRAY PYROLYSIS METHOD AND INFLUENCE OF ANNEALING PROCESS ON THEIR PROPERTIES

Mohammad Reza Khanlary[1] , Farnia Rashvand[2]
[1,2]Imam Khomeini international university,Department of physics,Ghazvin,Iran

Abstract- Transparent semiconducting Al-doped ZnO thin films were prepared on silicon substrates by spray pyrolysis method followed by in air annealing at 450°C. Zinc acetate dehydrate, 2-methoxyethanol and aluminum nitrate were used as a starting material, a solvent and a dopant source, respectively. X-ray diffraction patterns show that annealing process improves the crystallinity of the Al doped ZnO thin films .The mechanism of blue-green luminescence of AZO thin film are analyzed. Energy-dispersive X-rays (EDX) were used to analysis the composition of Al doped ZnO films. The morphology of the AZO thin films is studied by atomic force microscopy and FE-SEM analysis. Average diameter of some also obtained nanorods is ~60 nm.

Keywords - Spray pyrolysis; Al doped ZnO; Nanorods; photoluminescence; X-ray diffraction; morphology properties

I. INTRODUCTION

Zinc oxide (ZnO) is one of the most attractive II–VI semiconductor oxide materials, because of its wide resistivity range (10^{-4}–10^{12} Ω·cm) (Kyung Ho Kim et al., 2014) [1-6], direct wide band gap (3.37 eV) and large exciton binding energy (60meV) at room temperature. As a wide band gap oxide semiconductor, ZnO is an ideal material for ultraviolet (UV) optoelectronic applications. ZnO can be doped with various Group-III elements such as B, Al, Ga and In to induce n type conductivity. The existence of various ZnO nanostructures (nanoparticles, nanowires, nanorods (NRs), plate-like, flower-like, *etc*.) has expanded their use in many devices, such as thin film transistors (TFTs), field emission devices, solar cells, chemical sensors and acoustic devices (Kyung Ho Kim et al., 2014) [4-8].There are several deposition techniques that have been employed to grow undoped and doped ZnO thin films like chemical Vapor deposition (CVD) [9], magnetron sputtering [10], pulsed laser deposition (PLD) [11, 12], sol–gel process [13] and spray pyrolysis (SP) [14, 15]. On the other hand, chemical deposition techniques have received considerable attention due to the fact that large areas can be deposited at a low cost in an easy and safe. As a matter of fact, the chemical spray technique has been shown successful in the deposition of conductive and transparent oxides way (H. Gomez et al.,2007) [16]. Hence, further on we only refer to chemically sprayed ZnO thin films It is worthy to mention that among all the III Group, Al is a cheap, abundant and non-toxic material and can be an ideal candidate in replacing In if optimization of the process Deposition can be reached (H. Gomez et al.,2007). The spray pyrolysis technique is quite simple and the required set-up is less expansive and flexible for process modifications (A. El hichou et al., 2004). The ZnO doping is achieved by replacing Zn^{2+} atoms with atoms of elements of higher valance such as In^{3+}, Al^{3+}, Sn^{4+}, Pb^{4+} [1].

Additionally, by using this technique one can produce large area films without the need of a high vacuum and the Produced films can be controlled step by step (H. Gomez et al.,2007). In this work, Al-doped zinc oxide nanorods (NRs) are fabricated by spray pyrolysis. Although many studies concerning chemically-sprayed AZO thin films are reported in the literature, a lack of information exists concerning the variations in some of the deposition variables. This is the case of the Zn source, as it is usual the deposition of AZO thin films starting from zinc acetate and Al Nitrate ($Al(NO_3)_3$) as the dopant sources (H. Gomez et al.,2007). [6-10].Also The structural, morphological and photoluminescence properties of this films before and after annealing process is studied and reported.

II. EXPERIMENTAL DETAILS

A spray pyrolysis system used to obtain the films. Aqueous solutions of zinc acetate (C4H6O4Zn·2H2O) were used as ZnO precursors, and aluminum nitrate (Al (NO3)3)) were used as Al precursors. All the used solutions were 0.1M. The Al/Zn atomic ratio in the solution was 1%. During the deposition, the nozzle was 25 cm over the substrate. Compressed air was used to atomize the solution through a spray nozzle, over the heated substrate held at 400°C temperature. The solutions were pumped into the airstream by means of a syringe pump at a rate of 31 cm3/h [17-19]. The deposition time was varied between 40 to 75 min. p and n type Silicon (400) substrates of 1 cm×1 cm were uniformly coated (R. Romero et al., 2006) .

Publication History
Manuscript Received : 5 October 2014
Manuscript Accepted : 20 October 2014
Revision Received : 25 October 2014
Manuscript Published : 31 October 2014

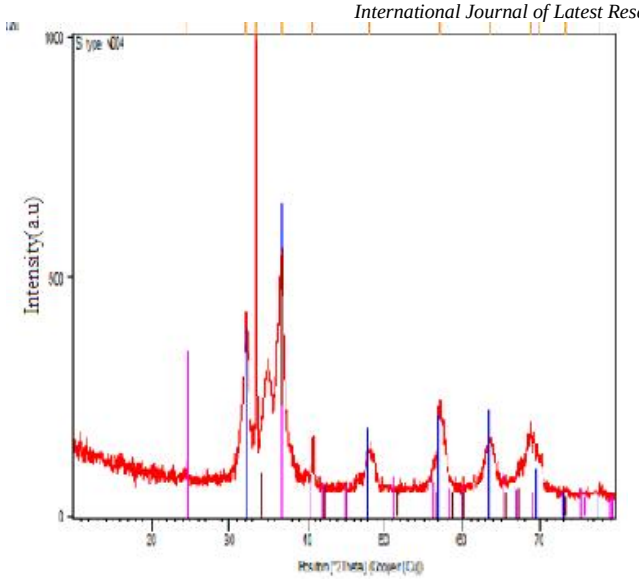

Fig. 1 XRD patterns of Al-doped ZnO thin films prepared with [Al]/[Zn] ratios at.1% and annealed at 450°C

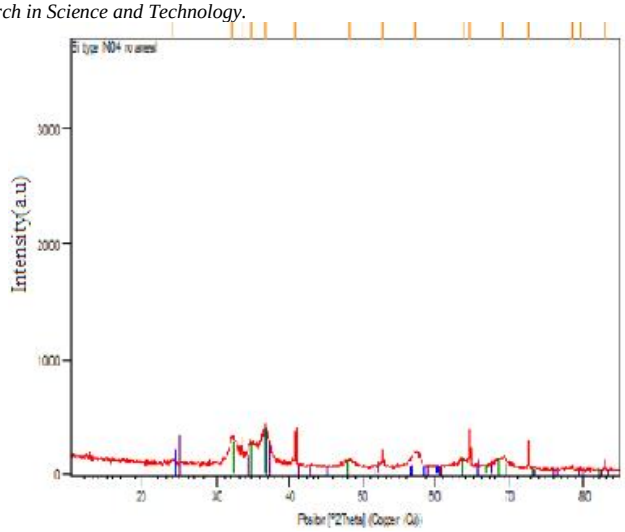

Fig. 2 XRD patterns of non-annealed Al-doped ZnO thin films prepared with [Al]/[Zn] ratios at.1%

III. STRUCTURAL PROPERTIES

The X-ray diffractograms of prepared AZO films at 400 C on p-type Si,(400), with both conditions of annealed at 450°C for 60 min and non-annealed with thickness of 380 nm were investigated. The x-ray diffraction (XRD) was used to investigate the structure of AZO thin films. The diffraction patterns were recorded by using a X 'Pert PRO model PW3050/60 XRD system with Cu-Kα radiation, and with Grazing measurement program operated at 40 kV and 40 mA, with angular range $10° \leq 2\theta \leq 100$.The XRD patterns of annealed AZO thin films depicted that all the films were polycrystalline in nature and of hexagonal wurtzite structure Furthermore, for the AZO films The trend of FWHM values indicated that the crystallinity of the films was improved with annealing (Joydip Sengupta et al., 2012). It was also observed (Table 1) that average grain size was augmented with annealing temperature for AZO films. This could be explained by considering the annealing induced coalescence of small grains by grain boundary diffusion which resulted in major grain growth. By annealing process, the grains become denser and larger which can be considered the coalescence process induced from thermal treatment [20]. For ZnO nanoparticles, there are many frenkel defects, such as Zn interstitials and oxygen vacancies at the grain boundaries (Min-Chul Jun et al., 2013) [20]. The crystallite size (l) of the ZnO:Al thin films was estimated from the X ray diffraction spectra based on the full-width measured at half-maximum (FWHM) of the (002) peak, using the Scherrer Eq(1):

$$D=k\lambda/B\cos\Theta \quad (1)$$

where λ is the wavelength of the Cu Kα1 radiation λ=0.15406 nm, B is FWHM of the diffraction peak measured in radians and θ is the corresponding diffraction angle. The grain growth mechanism includes the transfer of atoms at grain boundaries from one grain to another and the final grain size depends upon the specific annealing conditions (Joydip Sengupta et al., 2012). .

TABLE 1 ANNEALING PROPERTIES

sample	Annealing temperature	Annealing time	The average size of the grain by XRD(nm)
1.at% AZO/Si	450°C	60mins	20
1.at% AZO/Si	Non-annealed	----------	18.4

IV. MORPHOLOGICAL PROPERTIES

Figures 3 and 4 are a typical AFM surface images of an AZO Film of annealed AZO at 450 C and non-annealed respectively (table 2). AFM results indicate that the root-mean-square surface roughness and the average surface particle size. for annealed sample are 14.46 and 59 nm, respectively and for non-annealed sample are 5.71 and 40 nm. It indicates that with annealing process the RMS and the size of the grain is increased. The second reason, therefore, is that the polycrystalline AZO film deposited by SP has large surface roughness and surface particle size Pin-Chuan Yao et al., 2010). also the histogram show that the mean Ht for annealed sample and none annealed sample is 58.49 nm and 42.37 nm.

In a thin film solar cell, AZO NRs play the roles to extract carriers from the absorber and provide a fast and direct path for these carriers. The efficiency of a solar cell strongly relies on the crystallinity, density, diameter,and length of AZO NR [21]. when two bending NRs cross, the opposite charges will lead to the attraction at the crossed position due to the large electrostatic force one can see that the measured grain sizes from AFM are bigger than the ones derived from XRD data. This is because of the limitation of AFM to resolve smaller crystallites within a bigger grain (Mohit Kumar et al., 2013) [22, 23].

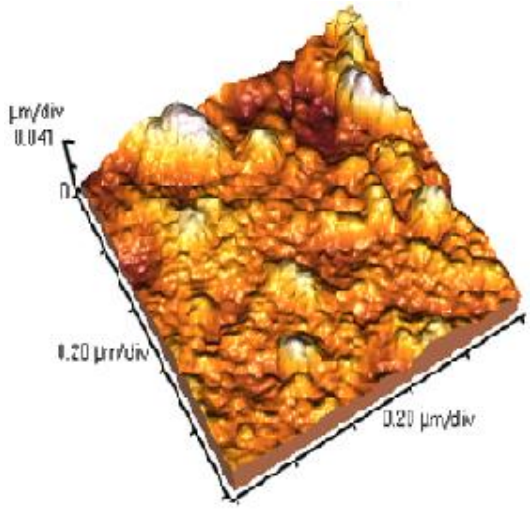

Fig 3. AFM image of annealed AZO thin film at 450°C

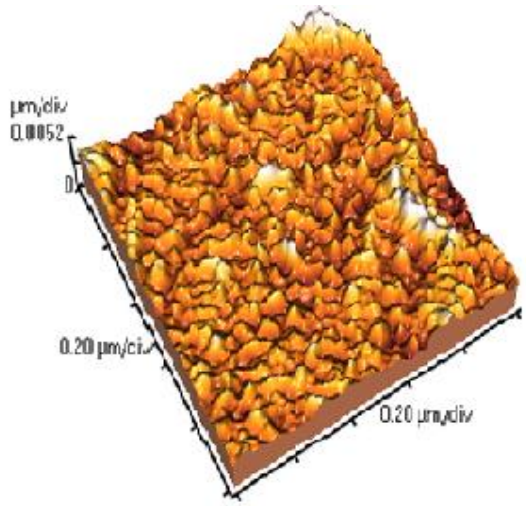

Fig 4. AFM image of non-annealed AZO thin film

TABLE 2 the average grain size by AFM

sample	Annealing temperature	Annealing time	The average size of the grain by AFM(nm)
1.at% AZO/Si	450°C	60mins	59
1.at% AZO/Si	Non-annealed	----------	40

Figures 5 and 6 and 7 show FE-SEM images of air-annealed the AZO NRs and thin films grown on the Si (400) substrate by using the SP method. Figs 6 and 7 shows non-annealed AZO thin films. Fig 5 shows cross sections of the NRs and thin film of annealed AZO nanorods at 450°C. The annealed grown AZO NRs had average length of about 400 nm On the other hand, the AZO NRs average diameter is about 60 nm. NRs are one morphology of nanoscale objects. They may be synthesized from metals or semiconducting materials. Standard aspect ratios (length divided by width) are 3-5.These vertical NRs arrays are highly suitable for use in solar cells [24]. This will make the solar cells more efficient at converting the solar energy that is directed at them. First, the rod diameter, length, spacing, and orientation are appropriate for forming a high-performance bulk hetero junction by filling the vertical array with a semiconducting polymer. In films, nucleation can be facilitated by the presence of the substrate, which constitutes a site for heterogeneous nucleation (Jong-Pil Kim et al., 2010) .The diffusion and hopping distance are dependent on substrate temperature. The grain size of the annealed and non-annealed films is shown in (table 2). And is comparable obtained grain size from XRD measurements (table 1). At the temperature of 400 C, the film had respective stoichiometry ratio between Zn and O which leads to the well crystallinity and thus to the large grain size. It can be seen that, with the annealing temperature of 450 C, the grain size is increased and more voids are presenting the film (Chongmu Lee et al., 2006).

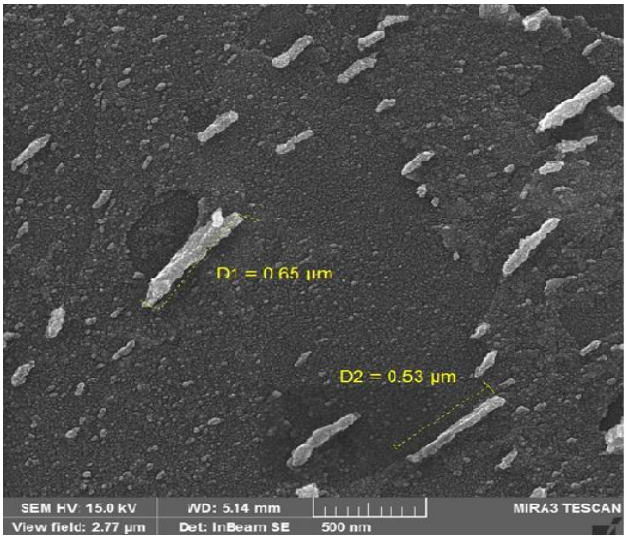

Fig 5. FE-SEM cross-section image of annealed AZO NRs And thin film

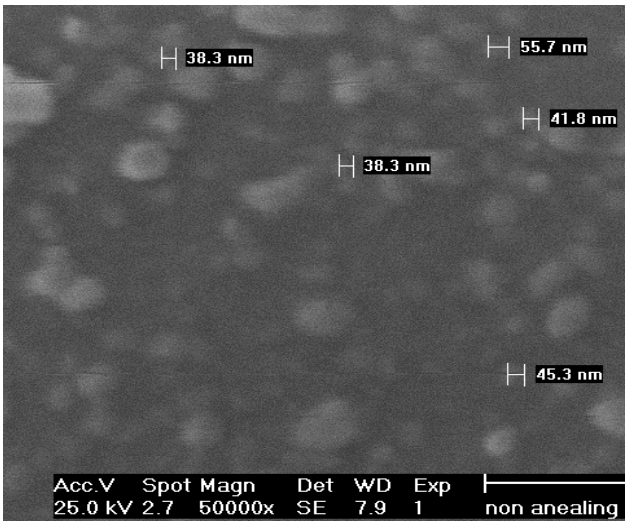

Fig 6. FE-SEM image of non-annealed AZO thin film

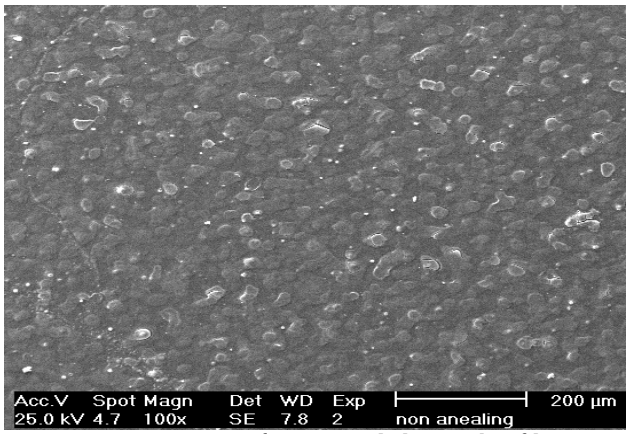

Fig 7. FE-SEM image of non-annealed AZO thin film

V. EDX SPECTRA

Figures 8 and 9 show the energy-dispersive X-ray spectrum of 1 % AZO film. The spectrum reveals the presence of Zn, O and Al elements in the deposited films. The silicon signal appears from the substrate. The presence of the Zn L_α peak at about 1.012keV, the Al K_α peak at 1.670keV and the O K_α peak at 0.450keV could be observed in the spectra. The table shows the related information about wt%, At%, k-ratio, and ZAF correction of annealed AZO and non-annealed AZO thin films respectively. According to this information, a change is obtained between percent of annealed and non-annealed AZO thin films. And this result follows the investigated information of XRD analysis. The energy of the X-rays that can be generated through inelastic scattering is characteristic for the energy levels of the elements present in the sample. By scanning the energy of the emitted X-rays, if the electron beam knocks out an inner shell electron of a sample atom (Elin Hammarberg et al), the vacancy is filled by an outer electron, and the excess energy is released as X-ray radiation.The transitions are named K-series, L-series, etc. after the shell of the knocked-out electron [25, 26]. EDAX can also be used for quantitative elemental analysis of the sample if a suitable calibration procedure has been adopted Since calibration standards consist of pure elements, whereas investigated samples normally are compounds, corrections of atomic number (*Z*), absorption (*A*), and fluorescence (*F*) effects must be carried out (so-called *ZAF* correction). The ZAF is investigated in these figures (Elin Hammarberg et al) .

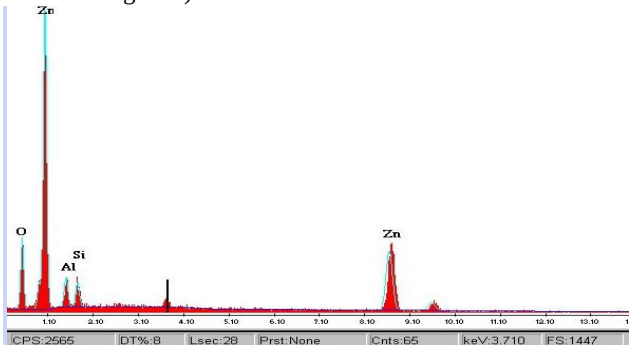

Figure 8. EDAX spectra of annealed AZO thin film

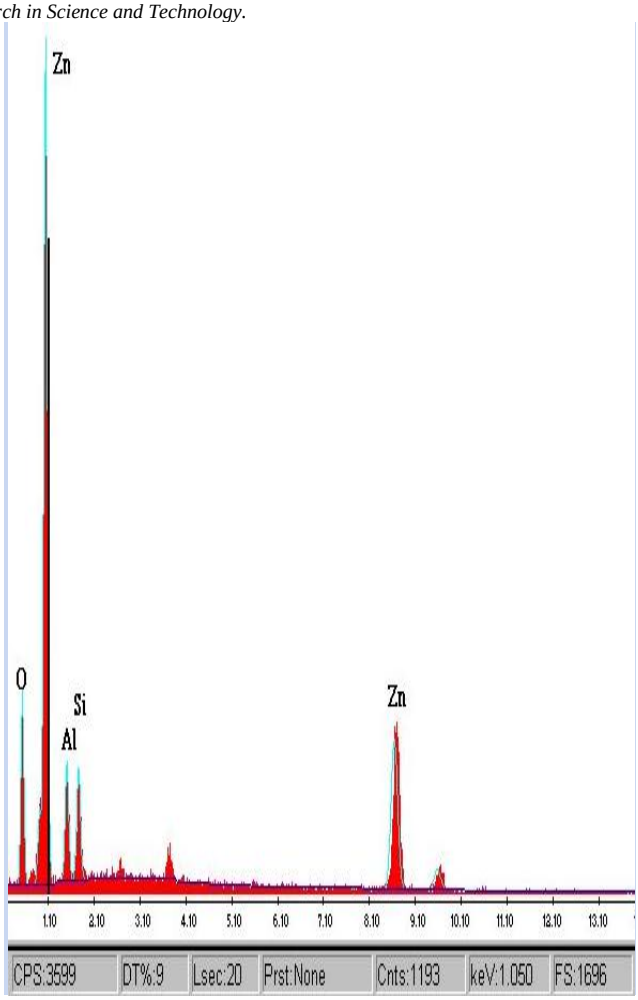

Figure 9. EDAX spectra of non-annealed AZO thin film

VI. PHOTOLUMINESCENCE SPECTRA

Figures 10 and 11 show the room-temperature PL spectra of the AZO as a function of the photon energy for the Al doping ratio. As shown in Figure 10, the PL spectra of the AZO with annealed conditions exhibited a near band-edge (NBE) at about 3.02 eV (UV region) and a deep-level emission centered at around 2.72 eV (blue-green region) (Pin-Chuan Yao et al., 2010).

.and for non-annealed 2.97 and 2.75 is exhibited respectively. The green band at around 2.4ev and the other one is located in the energy range 2.5 eV. The intensity of the green band increases significantly with annealing time [27, 28]. Oxygen vacancy, oxygen interstitial, zinc vacancy, and impurity are considered to be possible origins for these bands (Y.G. Wang et al., 2003). The near-band-edge (NBE) emission, which was generated by the free exciton recombination at about eV is showed. The green DLE originates from the recombination of the holes when electrons are observed to occupy the singly ionized oxygen vacancy (V_O^+) (Y.G. Wang et al., 2003) [29].

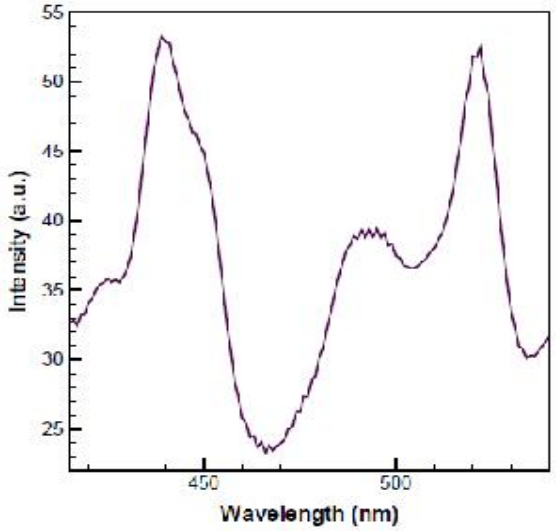

Figure 10. photoluminescence spectra of annealed AZO thin film at 450°C

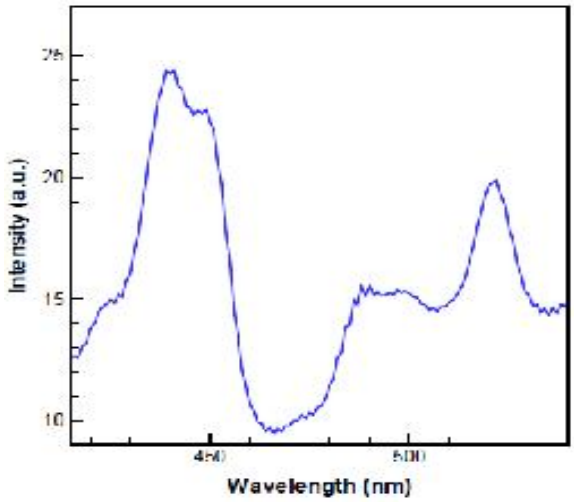

Figure 11. photoluminescence spectra of non- annealed AZO thin film

VI. CONCLUSION

In summary, we have fabricated AZO NRs by depositing a layer of AZO thin film on Si substrate using the spray pyrolysis technique. Influences of Al doping and an annealing treatment on structural and morphological and luminescence properties of AZO thin films were studied. The XRD spectra indicate that the films are of polycrystalline nature. It is clear that the morphology and grain size of the AZO thin films is influenced by the deposition conditions and annealing process. The EDX spectra and FE-SEM analysis confirmed the presence of aluminum in this composition and AZO NRs structure respectively. Photoluminescence spectra exhibited the region of NBE and DLE emission and confirmed the influence of annealing process on green band.

REFERENCES

[1] Mujdat Caglar, Saliha Ilican , Yasemin Caglar ,Springer, J Mater SciI: Mater Electron (2008) 19:704–708.

[2] Janotti, A.; van de Walle, C.G. Fundamentals of zinc oxide as a semiconductor. Rep. Prog. Phys. 2009, 72, 126501–126529.

[3] Kumar, B.; Kim, S.-W. Energy harvesting based on semiconducting piezoelectric ZnO nanostructures. Nano Energy 2012, 1, 342–355.

[4] Sun, Y.; Seo, J.H.; Takacs, C.J.; Seifter, J.; Heeger, A.J. Inverted polymer solar cells integrated with a low-temperature-annealed sol-gel-derived ZnO film as an electron transport layer.Adv. Mater. 2011, 23, 1679–1683.

[5] Park, K.; Lee, D.-K.; Kim, B.-S.; Jeon, H.; Lee, N.-E.; Whang, D.; Lee, H.-J.; Kim, Y.J.; Ahn, J.-H.Stretchable, transparent zinc oxide thin film transistors. Adv. Funct. Mater. 2010, 20, 3577–3582.

[6] Tsay, C.-Y.; Fan, K.-S.; Wang, Y.-W.; Chang, C.-J.; Tseng, Y.-K.; Lin, C.-K. Transparent semiconductor zinc oxide thin film deposited on glass substrates by sol-gel process. Ceram. Int.2010, 36, 1791–1795

[7] Kyung Ho Kim *, Kazuomi Utashiro, Yoshio Abe and Midori Kawamura, Materials **2014**, 7, 2522-2533

[8] Wang, X.; Song, J.; Summers, C.J.; Ryou, J.H.; Li, P.; Dupuis, R.D.; Wang, Z.L. Density-controlled growth of aligned ZnO nanowires sharing a common contact: A simple, low-cost, and mask-free technique for large- scale applications. *J. Phys. Chem. B* **2006**, *110*, 7720–7724.

[9] T.B. Asafa, N. Tabet, S.A.M. Said, Neuro computing 106 (2013) 86-94.

[10] D.K. Kim, H.B. Kim, Journal of Alloys and Compounds 509 (2011). 421-425.

[11] A. Suzuki, T. Matsushita, N. Wada, Y. Sakamoto, M. Okuda, Jpn. J.Appl. Phys. 235 (1996) L56.

[12] M. Miramatsu, K. Imeda, N. Horio, M. Nawata, J. Vac. Sci. Technol.A 16 (1998) 669.

[13] K. Lin, P. Tsai, Mater. Sci. Eng. B-Solid 139, 81 (2007).

[14] S.M. Rozati, Sh. Akesteh, Mater. Charact. 58, 319 (2007).

[15] H. Go´mez, A. Maldonado, R. Castanedo-Pe´rez, G.Torres-Delgado,M. de la L. Olvera, Mater. Charact. 58, 708 (2007).

[16] Ratheesh Kumar PM, Sudha Kartha C, Vijayakumar KP, Singh F,Avasthi DK. Effect of fluorine doping on structural, electrical andoptical properties of ZnO thin films. Mater Sci Eng B Solid-StateMater Adv Technol 2005;117:307–12.

[17] F.K. Shan, Y.S. Yu, J. Eur. Ceram. Soc. 24 (2004) 1869.

[18] R.Ayouchi, F.Martin, J.R.Ramos-Barrado,M.Martos, J.Morales,L. Sanchez,J. Power Sources 87 (2000) 106.

[19] R. Romero , D. Leinen , E.A. Dalchiele , J.R. Ramos-Barrado , F. Martín , Thin Solid Films 515 (2006) 1942–1949.

[20] C.S. Garret, T.B. Massalski, Structure of Metals, Pergamon Press, Oxford, 1980.

[21] (Conradt J, Sartor J, Thiele C, Flaig FM, Fallert J, Kalt H, Schneider R,Fotouhi M, Pfundstein P, Zibat V, Gerthsen D: Catalyst-free growth of zinc oxide nanorod arrays on sputtered aluminum-doped zinc oxide for photovoltaic applications. J Phys Chem C 2011, 115:3539–3543).

[22] S. Y. Hu, Y. C. Lee, J. W. Lee, J. C. Huang, J. L. Shen, and W. Water, Appl. Surf. Sci. **254**, 1578–1582 (2008).

[23] Kyung Ho Kim , Kazuomi Utashiro, Yoshio Abe and Midori Kawamura, Materials, 7, 2522-2533 (2014).)

[24] B. Postels, A. Kasprzak, T. Buergel, A. Bakin, E. Schlenker, H.-H. Wehmann and A. Waag, J. Korean Phys. Soc. 53, 115 (2008).

[25] S.R. Hejazi, H.R.M. Hosseini, M.S. Ghamsari, Journal of Alloys and Compounds 455 (2008) 353-357.

[26] H. Yumoto, T. Sako, Y. Gotoh, K. Nishiyama, T. Kaneko, Journal of Crystal Growth 203 (1999) 136-140.

[27] A.E. Jimenez-Gonzalez, J.A.S. Urueta, R. Suarez-Parra, J. Cryst. Growth 192(1998) 430.

[28] S.W. Xue, X.T. Zu, W.G. Zheng, M.Y. Chen, X. Xiang, Physica B 382 (2006) 201.

[29] K.E. Lee, M.S. Wang, E.J. Kim, S.H. Hahn, Curr. Appl. Phys. 9 (2009) 683.